Ekoloji 28(107): 789-796 (2019)

Multi-fracture Propagation Law of Horizontal Wells under Stress Shadow Effect

Kangxing Dong [1], Suling Wang [1*], Jinbo Li [1]

[1] Northeast Petroleum University, College of Mechanical Science and Engineering, 163318, Daqing, CHINA

[*] Corresponding author: wsl19751028@163.com

Abstract

In order to explore the law of multi-fracture propagation in cluster fracturing of horizontal wells, considering the stress shadows between fractures, a similarity numerical model for full three-dimensional fluid-solid coupling hydraulic fracturing was established, and the extended finite element method was used to solve the problem. The effects of rock mechanics properties, fracture interval and construction parameters on fracture propagation law were analyzed by the control variable method. The results show that with the increase of elastic modulus, the width of fractures on both sides and intermediate fractures decreases, while the length of multi-fractures increases. With the increase of displacement, the width of fractures on both sides increases first and then decreases, the width of intermediate fractures decreases first and then increases, the length of fractures on both sides increases gradually, and the length of intermediate fractures decreases slightly. With the increase of fracture interval, the width of fractures on both sides and in the intermediate increases little, but the length increases obviously. When the interval exceeds 30 m, the interaction between fractures is very small, and the fractures show a trend of parallel propagation. The research content of this paper has guiding significance for optimizing cluster interval in staged fracturing.

Keywords: stress shadows, horizontal wells, multiple fractures, extended finite element method

Dong K, Wang S, Li J (2019) Multi-fracture Propagation Law of Horizontal Wells under Stress Shadow Effect. Ekoloji 28(107): 789-796.

INTRODUCTION

Volume fracturing in horizontal wells is a key technology for effective development of unconventional reservoirs. Complex multi-fracture systems can be formed in reservoirs through volume fracturing to improve permeability (Chen et al. 2014, Warpinski et al. 2008, Wu et al. 2011). However, in volumetric fracturing, hydraulic fractures interfere with far-field stress, resulting in unbalanced development of hydraulic fractures and affecting the fracturing effect, which is called "stress shadow effect" (Xu et al. 2016). The key to solve this problem is to clarify the mechanism and variation law of stress shadow, which plays an important role in optimizing the construction parameters of volume fracturing and improving the effect of volume fracturing.

Since Sneddon (1946) first studied the distribution of stress field around a single fracture and gave the theoretical basis of stress shadow, the influence of stress shadow effect on fracture propagation has attracted the attention of scholars at home and abroad. At present, in the practice of shale gas development, it is found that the fracture will be turned within a certain range of existing fractures (Roussel and Sharma 2011, Qu et al. 2017). In theory, the analytical model of fracture induced stress is often used, which can calculate the induced stress (Xia et al. 2016) produced by opening the fracture in the plane of fracture height, but it cannot solve the stress change at any position of the wellbore. Previous studies mainly focused on the interaction between two fracture propagation under static conditions. The mechanism and regularity of stress shadows are still unclear, and the law of fracture initiation and propagation cannot be solved. Field practice has proved that reasonable use of stress shadow effect is the key to maximize the effect of artificial fracturing (Cai et al. 2014). Therefore, in this paper, numerical simulation technology was used to establish a full three-dimensional local stress model for multi-fracture propagation in horizontal wells. Considering the cumulative effect of borehole pressure, perforation and open fracture on in-situ stress near wellbore zone, the mechanism and regularity of multi-fracture initiation pressure were discussed, and the relationship between multi-fracture initiation pressure and design parameters was given, which provided theoretical support for volume fracturing design.

 Received: 20 Aug 2017 / Accepted: 5 Mar 2018

EXTENDED FINITE ELEMENT METHOD

The basis of XFEM is unit decomposition. The core idea of XFEM is to represent the discontinuity in the element by using the extended form function basis with discontinuity property. Therefore, in the process of calculation, the description of discontinuity field is completely independent of the grid, and it is not necessary to re-divide the grid when simulating fracture growth.

Extended Finite Element Model of Hydraulic Fracturing

In order to realize fracture analysis, the asymptotic function and discontinuous function near the fracture tip are added to the conventional finite element displacement model to describe the discontinuous displacement field.

$$u = \sum_{I=1}^{N} N_I(x)[u_I + H(x)a_I + \sum_{\alpha=1}^{4} F_\alpha(x)b_I^\alpha] \quad (1)$$

where,

$N_I(x)$=Displacement shape function of conventional nodes;

u_I= Continuous part of finite element displacement solution;

$H(x)$= Discontinuous jump function of fracture surface;

a_I, b_I^α=Node extended freedom vectors;

$F_\alpha(x)$=Fracture tip stress asymptotic function.

Consider that a rock matrix Ω_0 with hydraulic fractures, whose boundary is denoted as Γ_0, Γ_0^c as hydraulic fractures, Γ_0^u as displacement boundary and Γ_0^t as load boundary. The normal vectors of the hydraulic fracture surface are n^+ and n^- respectively, and the hydraulic pressure acting on the surface is p^+ and p^- respectively.

The boundary condition and initial condition are

Displacement boundary condition: $u = \bar{u}$, on the Γ_0^u.

Load boundary condition: $\sigma \cdot n = \bar{t}$, on the Γ_0^t

For the fracture in the matrix, the condition that the surface force is zero on the fracture surface:

where,

σ =Cauchy stress tensor, Pa;

n=Unit normal vector;

$\bar{u}$=Displacement on the Γ_0^u, mm;

$\bar{t}$=Surface force on the Γ_0^u, N.

The equilibrium equation of hydraulic fracturing rock mass is as follows:

$$\nabla \cdot \sigma + b = \rho\ddot{u} \quad (2)$$

where,

b =Physical strength per unit volume, N;

ρ =Density of liquid, Kg/m^3;

$\ddot{u}$=Accelerated speed, m/s^2.

The constitutive equation for isotropic materials is:

$$\sigma = C:\varepsilon \quad (3)$$

where,

ε =Strain tensor, m;

C =Elasticity tensor, Pa/m.

For the strong form of the problem multiplied by a possible displacement, the weak form of the equilibrium equation can be obtained as follows:

$$\int_{\Omega_0} \sigma \cdot \varepsilon d\Omega_0 = \int_{\Omega_0} b \cdot u d\Omega_0 + \int_{\Omega_0} \rho\ddot{u} \cdot u d\Omega_0 + \int_{\Gamma_0} \bar{t} \cdot u d\Gamma_0 \quad (4)$$

where,

u =Virtual displacement, m.

The above formula is the virtual work equation of hydraulic fracturing. By substituting the displacement field formula 1 of extended finite element into the upper formula, the equilibrium equation of extended finite element of hydraulic fracturing can be obtained.

The length of the hydraulic fracturing fracture is much larger than the fracture width. Therefore, the liquid flow in the fracture width direction can be neglected. Considering only the flow of the fracturing fluid along the fracture propagation direction, the fluid flow control equation can be obtained according to the Reynolds theory and the mass conservation theory:

$$\frac{\partial p}{\partial s} = -\frac{12q}{w^3}, \frac{\partial p}{\partial s} + \frac{\partial w}{\partial t} = 0 \quad (5)$$

where,

q=Cross-sectional flow, m^3/s;

w=Width of fracture, m;

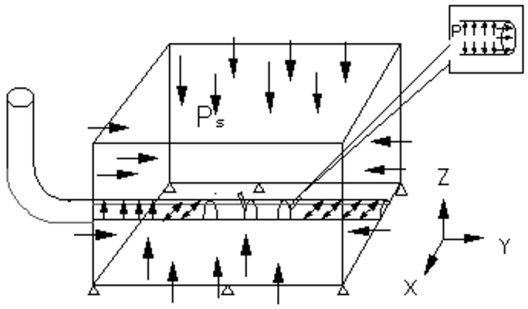

Fig. 1. Mechanics Model

s=Displacement along the fracture propagation path;

μ=Fluid viscosity, Pa└s.

The conservation equation of fluid mass is:

$$Q_0 \Delta t = \int_0^L \Delta w ds \tag{6}$$

Fracture Initiation Criterion and Propagation Direction

In this paper, the maximum principal stress criterion was adopted for fracture propagation. When the maximum principal stress reached the critical stress at the integral point of the element (within a certain error range), new fracture or original fracture propagation would be introduced after the next incremental step.

When the fracture criterion was met, the newly introduced fracture was always perpendicular to the direction of maximum principal stress.

Flow of Liquid in Fractures

The flow of fluid in a fracture includes tangential flow along the fracture wall and normal flow along the vertical fracture wall.

Vector equation of volume flow density of Newtonian fluid in tangential flow:

$$qw = -k_t \nabla p \tag{7}$$

$$k_t = \frac{d^3}{12\mu} \tag{8}$$

where,

k_t=Flow resistance;

∇p =Pressure gradient on fracture surface.

The normal flow of fluids is the permeation of fluids in the matrix. The normal flow can be defined as:

$$q_t = c_t(p_i - p_t) \tag{9}$$

$$q_b = c_b(p_i - p_b) \tag{10}$$

where,

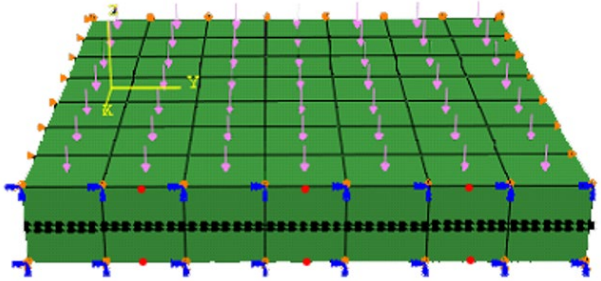

Fig. 2. Extended Finite Element Mechanics Model

q_t, q_b=Flow rate on the upper and lower surfaces of the flow fracture;

p_i=Fluid pressure in the fracture;

p_t, p_b=Pore pressure on the upper and lower surfaces.

MECHANICAL MODEL AND FINITE ELEMENT MODEL

In this paper, a symmetric extended finite element model (assuming that both flanks of a fracture develop symmetrically in the process of propagation) was established according to the fracturing situation in the field. The constraints were as follows: displacement constraints were applied to the bottom of Z direction, both sides of Y direction, one side of X direction, and symmetrical boundary was applied to the other side of X direction to simulate the displacement constraints of strata in three directions. The overlying pressure was applied in Z direction to simulate the pressure action of overlying rock on the analytical model. Gravity was applied to the whole model. Confining pressure and pore pressure were applied all around. Initial field stress was applied to three directions of the whole model to simulate the initial stress field caused by rock mass occurrence environment. Initial fractures were established and injected with a certain rate of fracturing fluid to simulate field fracturing. Using structured grid, the unit was divided into C3D8RP seepage type to simulate the fluid-solid coupling effect under seepage in real rock strata. The mechanical model and finite element model are shown in **Fig. 1** and **Fig. 2**. Because the geological conditions were very complex, in order to facilitate analysis and calculation, the following hypotheses were made when establishing the mechanical model of multi-fracture propagation:

(1) The physical and chemical interaction between rock and fracturing fluid is neglected.

(2) Fracturing fluid is completely saturated and incompressible.

Table 1. Similar Parameters Proportion for Similar Models

Length	Pressure	Speed	Void rate	Kinetic viscosity	Permeability
$\frac{L_p}{L_m}=\frac{1}{100}$	$\frac{P_p}{P_m}=\frac{1}{100}$	$\frac{U_p}{U_m}=\frac{10}{1}$	1	$\frac{\mu_p}{\mu_m}=\frac{1}{100}$	$\frac{k_p}{k_m}=\frac{100^2}{1}$

Table 2. Comparison of Similar Model and Original Model

	S_{11}/MPa	S_{22}/MPa	S_{33}/MPa	Fracture width/mm
Similar Model	-0.23	0.20	0.26	4.96
Original Model	23.42	19.71	25.87	5.01
Error	1.8%	1.5%	0.5%	1%

(3) Rocks are porous elastic media and homogeneous isotropic.

(4) The influence of formation temperature on fracture propagation is neglected.

SIMILARITY MODEL AND VERIFICATION

Fracture height and fracture length usually develop to about 100 meters. If an extended finite element model was established in a ratio of 1:1 and permeable meshes were divided, the requirement for computer was very high and the calculation time was unacceptable. In this paper, the similarity principle was used to optimize the modeling, and the model was simplified to a certain extent to reduce the error, so that the interaction between hydraulic fractures was more realistic and objective. According to the first theorem of similarity (Kong et al. 1996, Lin 1984), the proportion of parameters of similarity model is determined as shown in **Table 1**.

In order to verify the above derivation, the original model and the similar model were calculated separately. The original model size was 100 m×100 m×15 m, the initial ground stress was 24 MPa, 20 MPa, 26 MPa, and the pore pressure was 18 MPa. The similarity model size was 1 m × 1 m × 0.15 m, the initial ground stress was 0.24 MPa, 0.20 MPa, 0.26 MPa, and the pore pressure was 0.18 MPa. The element types of the original model and similar model were the same, and the initial fractures of the extended finite element method were given in the model. **Table 2** shows the results of similarity model and original model on the basis of similarity.

It is observed from **Table 2** that the comparison between the results of the similarity model and the original model shows that after the balance of ground stress, the formation of the three directions of ground stress and hydraulic fractures, the fracture propagation patterns were compared, and the error was within the allowable range, which proves that the full-three-dimensional extended finite element hydraulic multi-fracture model established by the similarity principle was reasonable.

ANALYSIS OF MULTI-FRACTURE PROPAGATION LAW

The main influencing factors of multi-fracture propagation are ground stress state, rock mechanics property, fracturing fluid property and construction parameters. In order to study the influence of the above factors on fracture propagation, the control variable method was adopted in this paper. On the premise that other parameters remained unchanged, only one of them was changed, the effect on fracture propagation was studied qualitatively.

Impact of Construction Displacement

Initial ground stress was set as σ_X=24 MPa, σ_Y=20 MPa, σ_Z=26 MPa, elasticity modulus as 30 GPa, porosity as 0.2, the displacements were 1.8 m^3/min, 2.4 m^3/min, 2.7 m^3/min and 3.0 m^3/min, respectively. When displacement was 2.7 m^3/min and 3 m^3/min, the propagation patterns of the three fractures are shown in **Fig. 3** and **Fig. 4**.

According to the analysis of the fracture propagation pattern, a fracture parallel to the X-axis will theoretically occur without considering the interaction between multiple fractures. However, in the process of multi-fracture propagation, there is stress shadow effect due to the interaction between fractures. The stress shadow produced by the two sides of the fracture inhibits the development of the intermediate fracture, which shows that the propagation of the intermediate fracture lags behind that of the two sides of the fracture for a period of time at the beginning of the fracturing. The increase of displacement leads to the increase of net pressure inside the fracture, and the seepage effect increases the pore pressure around the fracture and weakens the difference of ground stress. Therefore, the fracture propagation at both sides tends to increase with the increase of displacement and X-axis. Therefore, displacement has a certain effect on the bending degree of multi-fracture propagation. The larger displacement, the greater the acute angle between fracture and X-axis,

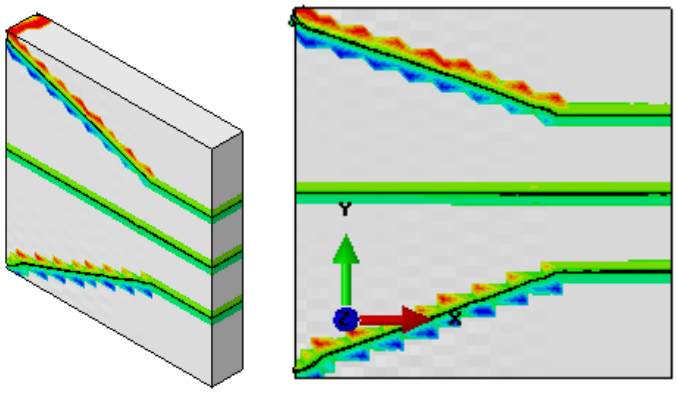

Fig. 3. Multi-fracture Propagation Patterns (flow rate as 2.7 m^3/min)

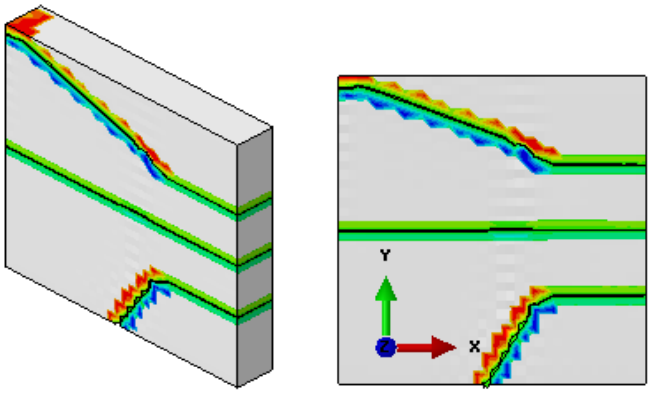

Fig. 4. Multi-fracture Propagation Patterns (flow rate as 3 m^3/min)

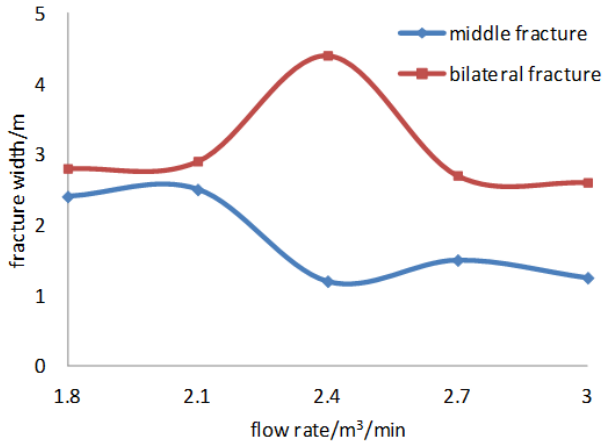

Fig. 5. Relationship between fracture width and flow rate

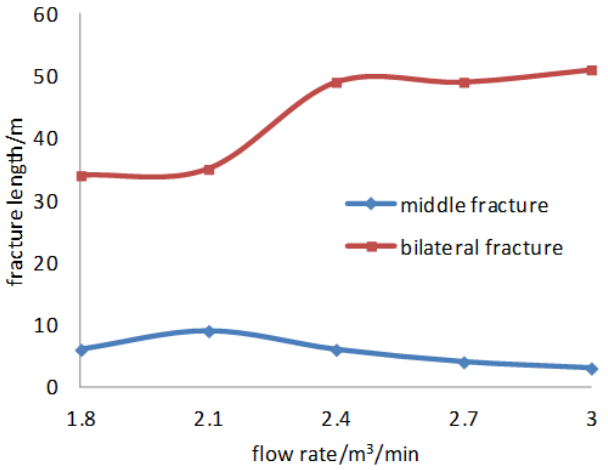

Fig. 6. Relationship between fracture length and flow rate

indicating that the influence of horizontal ground stress difference can be weakened by the increase of displacement in short distance.

With the increase of pump displacement, the width of fractures on both sides of multi-fractures increased first and then decreased, while the width of intermediate fractures decreased first and then increased slightly; the length of fractures on both sides increased gradually, while the length of intermediate fractures decreased slightly. When displacement increased from 1.8 m^3/min to 2.4 m^3/min, the width of fractures on both sides increased gradually while the width of intermediate fractures decreased gradually. The maximum increase of fracture width on both sides was 2.22 mm, and the intermediate decrease was 1.21 mm. The length of the fractures on both sides showed an increasing trend. When the displacement increased

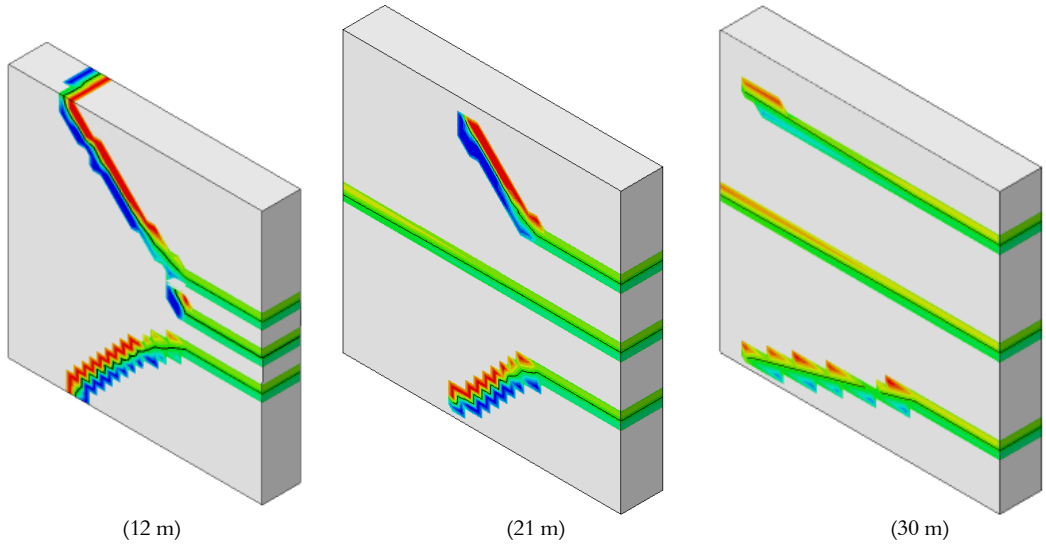

(12 m) (21 m) (30 m)

Fig. 7. Multi-fracture Propagation Patterns of different spacing

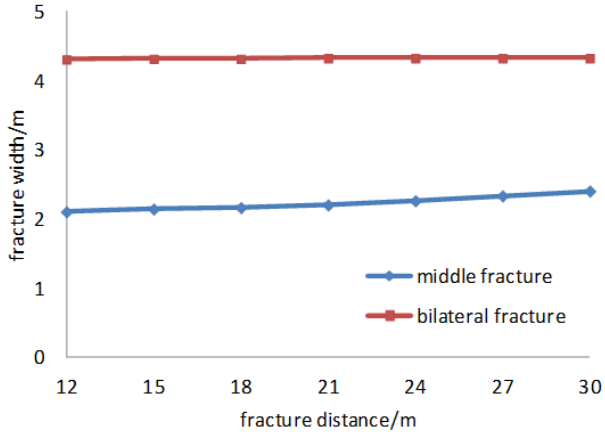

Fig. 8. Relationship between fracture width and distance

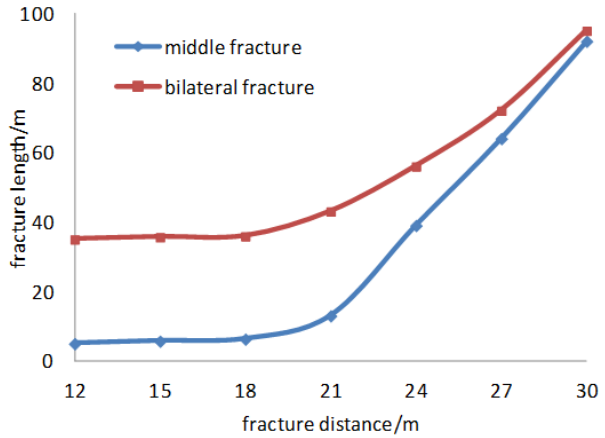

Fig. 9. Relationship between fracture length and distance

from 2.4 m^3/min to 3.0 m^3/min, the pressure amplitude in the fracture increased greatly, on the one hand, it exceeded the limit of rock bone strength, on the other hand, it could reach the rock tensile strength, which made the fracture expand forward continuously, and then caused the pressure drop in the fracture, which reduced the fluid loss in the normal direction of the fracture, thus weakening the increase in the width direction of the fracture. Compared with displacement of 2.4 m^3/min and 3.0 m^3/min, the width of fractures on both sides was only 0.14 mm different. With the increase of pump displacement, the ability of the intermediate fracture to resist the pressure stress of both sides of the fracture gradually increased, and the normal fluid loss in the fracture would also increase, which was the phenomenon when the displacement exceeded 2.4 m^3/min.

Effect of Fracture Interval

The initial ground stress was set as 24 MPa, 20 MPa and 26 MPa, elasticity modulus as 30 Gpa, permeability as 0.2 μm, average porosity as 0.2, displacement as 1.8 m^3/min, and fracture interval as 12 m, 21 m and 30 m. The trend of fracture propagation is shown in **Figs. 7**.

It is observed from **Fig. 8** to **Fig. 9** that with the increase of fracture interval, the trend of multi-fracture propagation tended to be parallel and the phenomenon of mutual exclusion decreased gradually, mainly because the increase of fracture distance caused the weakening of stress shadow between fractures. Therefore, when multi-cluster optimization of tight reservoir rocks was carried out, the distance between multi-clusters can be optimized within 30m under this formation condition.

Effect of Elastic Modulus

The initial ground stress was set as 24 MPa, 20 MPa and 26 MPa, fracture interval as 21 m, permeability as 0.2 μm, average porosity as 0.2, displacement as 1.8

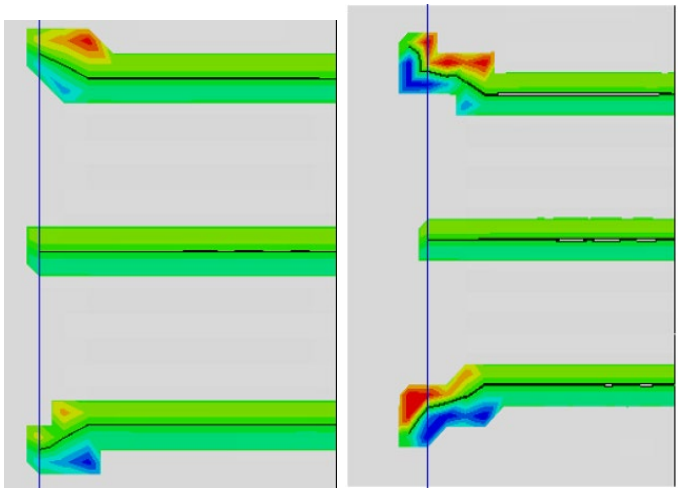

(10GPa) (40GPa)

Fig. 10. Multi-fracture Propagation Patterns of different spacing

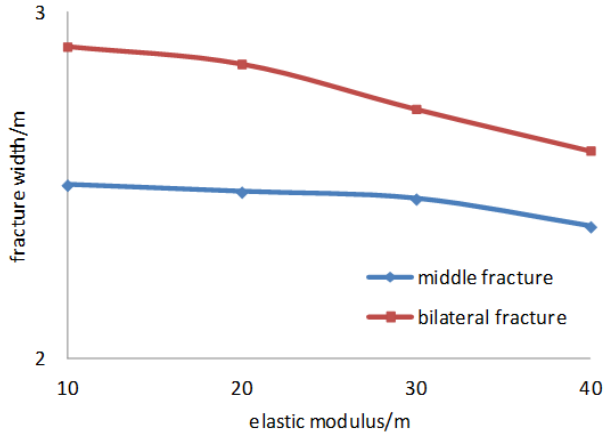

Fig. 11. Relationship between fracture width and elastic modulus

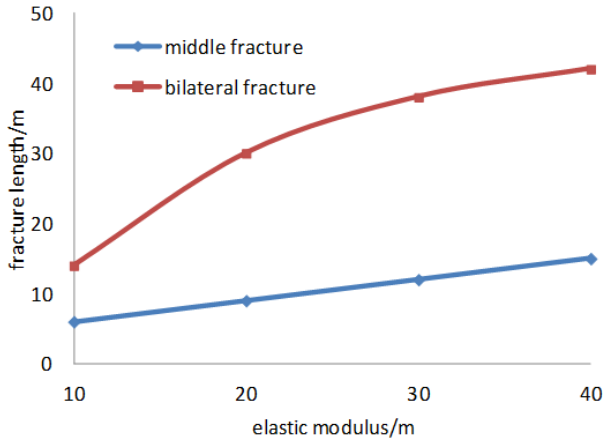

Fig. 12. Relationship between fracture length and elastic modulus

m^3/min, and elasticity modulus as 10 GPa, 20 GPa, 30 GPa and 40 GPa. The trend of fracture propagation is shown in **Figs. 10-12**.

With the increase of elastic modulus, the width of fractures on both sides and intermediate fractures decreased gradually, and the reduction range of fractures on both sides was larger than that of intermediate fractures; and the length of both sides and intermediate fractures increased gradually. This is because with the increase of elastic modulus, the restraining effect of the fractures at both sides on the intermediate fracture increased gradually, resulting in the decrease of the width and length of the intermediate fracture propagation. At the same time, the propagation of intermediate fractures lagged slightly for about 3.7m and 6.7m, indicating that when the modulus of elasticity was small, it was easy to produce short and wide fractures, and when the modulus of elasticity was large, it was easy to produce narrow and long fractures. The smaller the modulus of elasticity, the better the "elasticity" of the material, and it is easy for the material to expand in the radial direction.

CONCLUSIONS

In this paper, based on the extended finite element theory, the simulation method of three-dimensional hydraulic multi-fracture propagation of tight reservoir was established. Based on the analysis of the propagation patterns of multiple fractures under different formation conditions, the following conclusions are drawn:

(1) With the increase of displacement, the width of fractures on both sides increases first and then decreases, the width of intermediate fractures decreases first and then increases, the length of fractures on both sides increases gradually, the length of intermediate fractures decreases slightly, and the larger displacement,

the better the effect of in-situ stress difference can be overcome in the area near wellbore.

(2) With the increase of elastic modulus, the width of fractures on both sides and in the middle decreases, and the length of multi-fractures increases. The larger the elastic modulus, the easier it is to form short and wide fractures. The smaller the elastic modulus, the easier it is to form narrow and long fractures.

(3) With the increase of fracture interval, the width of fractures on both sides and in the middle increases slightly, but the length increases obviously. When the fracture interval is 30m, the interaction between fractures is very small, and the fractures show a trend of parallel propagation.

(4) Based on the above analysis, it is concluded that the variation of ground stress in multi-fracture is obviously affected by the interval, followed by displacement and elastic modulus.

ACKNOWLEDGEMENT

Youth Science Foundation of Northeast Petroleum University (2018QNL-01) and National Basic Research Program of China (973 Program, 2015CB250900).

REFERENCES

Cai B, Tang BZ, Ding YH, et al. (2014) Influence of stress shadow on horizontal well fracturing. Natural Gas Industry, 34(7):55-59.

Chen YJ, Zhang MJ, Li W, et al. (2014) A comparative analysis of investment and benefit between conventional fracturing and fracturing by stimulated reservoir volume (SRV): Cases history of gas/shale gas wells in the Southern Sichuan Basin. Natural Gas Industry, 34(10):128-132.

Kong YX, Lu DT, Xu XZ, et al. (1996) Study on convection in porous media. Advances in Mechanics, 26(4):510-520.

Lin YM (1984) Simulation study of experimental rock mechanics. Coal Industry Publishing House:3-17.

Qu ZQ, Tian Y, Li JX, et al. (2017) Numerical simulation study on fracture extension and morphology of multi-cluster staged fracturing for horizontal wells. Journal of China University of Petroleum (Edition of Natural Science), 41(1):102-109.

Roussel N, Sharma M (2011) Strategies to Minimize Fracture Spacing and Stimulate Natural Fractures in Horizontal Completions.

Sneddon NI (1946) The distribution of stress in the neighborhood of a crack in an elastic solid. Proceedings of the Royal Society a Mathematical Physical and Engineering Sciences, 87(2):229–260.

Warpinski NR, Mayerhofer MJ, Vincent MC, et al. (2008) Stimulating unconventional reservoirs: maximizing network growth while optimizing fracture conductivity. SPE 114173.

Wu Qi, Xu Y, Wang TF, et al. (2011) The revolution reservoir stimulation: An introduction of volume fracturing. Natural Gas Industry, 31(4):7-12.

Xia L, Zeng YW, Jin L, et al. (2016) Research on influence of initial horizontal principal stress on stress shadow. Chinese Journal of Rock Mechanics and Engineering, 35(1):2819-2825.

Xu Y, Chen M, Wu Q, et al. (2016) Stress interference calculation model and its application in volume stimulation of horizontal wells. Petroleum Exploration and Development, 43(5):128-132.